X-621-71-299
PREPRINT

X- 65660

TURBULENCE OF ELECTROSTATIC ELECTRON CYCLOTRON HARMONIC WAVES OBSERVED BY ALOUETTE-II AND OGO-V

HIROSHI OYA

JULY 1971

GSFC

GODDARD SPACE FLIGHT CENTER
GREENBELT, MARYLAND

TURBULENCE OF ELECTROSTATIC ELECTRON CYCLOTRON HARMONIC WAVES OBSERVED BY ALOUETTE-II AND OGO-V

Hiroshi Oya

ABSTRACT

VLF emissions which have been observed near $3/2f_H$, $5/2f_H$ and $7/2f_H$ by OGO-5 in the magnetosphere, where f_H is the electron cyclotron frequency, coincide with the most favorable point for long duration diffuse plasma resonances f_{Dn} observed by Alouette-2 and ISIS-1. The f_{Dn} are enhanced being associated with nonlinear wave particle interaction of the electrostatic electron cyclotron harmonic wave, including the instability in the turbulence. The difference between the two observations is only in the excitation mechanism of the turbulence; the turbulence in the plasma trough detected by OGO-5 is due to natural origins while the ionospheric topside sounder makes the plasma wave turbulence artificially by submitting strong stimulation pulses. An electron density profile in the plasma trough is obtained by applying the f_{Dn}-f_N/f_H relationship obtained from the Alouette 2 experiment; the values reveal a good coincidence with high sensitive mass-spectrometer observations which give values of $1 \times 10^{-1} \sim 5 \times 10^{-1}$ cm^{-3}.

TURBULENCE OF ELECTROSTATIC ELECTRON CYCLOTRON HARMONIC WAVES OBSERVED BY ALOUETTE-II AND OGO-V

1. INTRODUCTION

By observations of plasma resonances of Alouette-2 and VLF emissions of OGO-5, whose apparent features seem to be widely different from each other, a similar phenomenon was observed. In the Alouette-2 observation the sequence of diffuse plasma resonance f_{Dn} was discovered (Oya, 1970). This is a kind of plasma resonance which is represented by a prolonged signal in a certain period while the transmitter has been turned off following the transmission of the relatively high power RF pulse. The center frequency, or the frequency of the longest duration portion (for the asymmetrical resonances), f_{Dn} for these resonances is plotted in the f/f_H - f_N/f_H diagram (see Fig. 1) where f_H is the electron cyclotron frequency, f_N is the plasma frequency, and f_T is the upper hybrid resonance frequency. The electrostatic wave resonances f_{Qn} (Warren and Hagg, 1968) are also plotted in Fig. 1.

In the VLF electric field observation in the magnetosphere a new emission with frequency slightly above 1.5 f_H, which is expressed here as $f \gtrsim 1.5f_H$, has been observed by Kennel et al. (1970). This is a relatively strong emission with a field intensity of tens of mv/m, observed for several L values, within a few degrees of the geomagnetic equator. Furthermore it was found that this new type of magnetospheric emission is an electric field emission, and shows a sequence nature with a frequency separation of approximately f_H. For simplicity of expression these emissions will be designated as $(3/2)\ f_H$, $(5/2)\ f_H$ and $(7/2)\ f_H$. The August 15 events of OGO-5 VLF emissions (Kennel et al., 1970) are reproduced in Fig. 3.

The purpose of this report is to clarify that the above described VLF emissions are caused by a wave-particle nonlinear interaction in a turbulence of electrostatic electron cyclotron harmonic waves as it has been established for the case of the f_{Dn} resonances (Oya, 1971) that are observed by Alouette-2 and ISIS-1.

2. REVIEW ON f_{Dn} FORMATION MECHANISM

The applied power of the Alouette-2 satellite experiment is 300 Watt in a pulse form with 100 μsec width. The energy absorbed by the plasma depends on the frequency; the calculated energy (Oya, 1971) is from 6 to 260 times greater than the thermal energy of the plasma. This strong trigger pulse starts plasma turbulence in which a nonlinear interaction and a temperature anisotropy are involved. The observations (see Fig. 1) indicates that the f_{Dn}, f_{Qn+2} and $2f_H$ frequencies; and also the f_{Dn1}, f_{Qn+1} and f_H frequencies are related as:

$$f_{D1} = f_{Q3} - 2f_H \tag{1}$$

$$f_{D2} = f_{Q4} - 2f_H \tag{2}$$

$$f_{D11} = f_{Q2} - f_H \tag{3}$$

and

$$f_{D21} = f_{Q3} - f_H . \tag{4}$$

where f_{D11} and f_{D21} are weaker branches of the diffuse plasma resonances which occur in the upper frequency side of the main branch f_{D1} and f_{D2}, respectively (see Fig. 1). The main subject of the present paper is restricted to the occurrence of f_{D1} and f_{D2} given by Eqs. (1) and (2).

Using computed dispersion curves obtained for the electrostatic electron cyclotron harmonic wave starting from Stix's Eq. (18) of Chapt. 9 (1962), the validity of the three-wave nonlinear interaction condition,

$$f_{Dn} = f_{Qn+2} - 2f_H \tag{5}$$

and

$$\vec{k}\,(f_{Dn}) = \vec{k}\,(f_{Qn+2}) - \vec{k}\,(2f_H), \tag{6}$$

where $\vec{k}\,(f_{Q3})$, $\vec{k}\,(f_{D1})$ and $\vec{k}\,(2f_H)$ are the propagation vectors of the waves, is checked. These relations indicate also that

$$2\pi\,\{2f_H - (f_{Qn+2} - f'_{Dn})\} = \{\vec{k}\,(f_{Qn+2}) - \vec{k}\,(f'_{Dn})\} \cdot \vec{v}, \tag{7}$$

where f'_{Dn} is a resonant frequency that is in the band width of f_{Dn} resonance, since $\vec{k}\,(2f_H)$ is very close to zero. This equation corresponds to a wave-particle coupling near the $2f_H$ resonance. The resonant particles with velocity $\vec{v}$ which satisfy Eq. (7) effectively absorb energy from the waves and the temperature anisotropy, $T_\parallel/T_\perp < 1$, is established.

The temperature anisotropy produced by the high power supply of the Alouette-2 sounder, as mentioned above, causes the electrostatic electron cyclotron harmonic wave instability which was initially predicted by Harris (1959) for the extreme temperature anisotropy $T_\parallel/T_\perp = 0$, where $T_\parallel$ and $T_\perp$ are the temperature of the particle motions parallel and perpendicular to the magnetic field, respectively. The work was later extended by Hall et al. (1965), Terashima (1967) and Tataronis et al. (1969). These works were mainly concerned with the frequency range close to the cyclotron harmonic waves. A criterion for the instability condition was expanded to cover the whole frequency range by Shima and Hall (1965) using an analytical method, they predicted that the instability occurs in a range $n + 0.5 < f/f_H < n + (1 - T_\parallel/T_\perp)$. A more extensive numerical calculation to give the growth rate and the domain of the instability was carried out by Oya (1971). An example of the calculated instability is reproduced in Fig. 3, for the condition $T_\parallel/T_\perp = 0.2$ and $T_\parallel/T_\perp = 0.1$, respectively. The observation in the above paper also indicates that the most favorable condition for the instability clearly coincides with the longest time duration portion of the f_{Dn}.

The nonlinear process given by Eq. (7) can continue until the intensity of the initial disturbance reduces to the threshold level for the linear case. The nonlinear interaction can also exist independent of the instability. From Fig. 3 it is clear that the phenomena in the frequency range below $1.5f_H$ for f_{D1} are simply the result of nonlinear wave-wave interaction, because there is no instability region in the frequency range $f/f_H < 1.5$. In this case the duration time becomes shorter for the f_{D1} resonance than the case in which f_{D1} is in the region of the cyclotron harmonic wave instability. The whole mechanism described here will be published more in detail with substantial experimental evidence (Oya, 1971).

3. COMPARISON OF THE VLF EMISSIONS AND f_{Dn} RESONANCES

The observation of OGO-5 VLF emissions and of Alouette-2 diffuse plasma resonance f_{Dn} shows the following characteristics:

1. The main portion, which is defined as the longest portion or the most intense signal portion, reveals the sequence of appearance in the frequency range f according to

$$(n + 0.5)\, f_H < f < (n + \alpha)\, f_H \tag{8}$$

where α varies due to the plasma condition in a range $0.6 < \alpha < 1$.

2. The first member of this series of phenomena ($n = 1$ for the f_{Dn} resonance, and the $(3/2)\, f_H$ wave for the VLF emission) shows the strongest signal intensity or the longest duration time of all members of the series.

3. Both phenomena sometimes occur in a frequency range below $1.5 f_H$. This lower side expansion occurs, for the f_{D1} resonance, in a strict relationship with the plasma parameter (see Fig. 1). The lower side extension for the $(3/2)\, f_H$-wave emission, which occurs systematically in time, is suggesting the dependency on variation of local plasma parameters at the satellite location.

There are, however, remarkable differences between the two experiments: The Alouette-2 signal is excited by the transmission of an RF pulse and the phenomenon stops in 2 to 20 m sec after the transmission of the triggering pulse. In contrast, VLF emissions last up to tens of minutes, there is no sounding transmitter on board.

The band width of the VLF emission in the dynamic spectrum of the emission given in Fig. 2 is scaled being sampled every second (see Fig. 3) with the computed domain of the cyclotron harmonic wave instability for the temperature anisotropy of $T_\perp / T_\parallel = 5$ and $T_\perp / T_\parallel = 10$. Between 0727 :30 -0728 :00 UT, the instability region and the VLF emission band indicates complete coincidence in a temperature anisotropy $5 < T_\perp / T_\parallel < 10$. To maintain this relatively high temperature anisotropy the $2 f_H$ wave-particle nonlinear interaction has an important role in the hypothesis that the VLF emission and f_{Dn} are caused by the same mechanism. The nonlinear wave particle interaction can be confirmed by the record given in Fig. 3, i.e., there is an interval of no signal for the first sequence of the emission, i.e., (3/2) f_H-waves, between approximately 0727:54 to 0727:58 UT, though the second and the third sequence of the emissions exist. This is only possible when the nonlinear coupling to satisfy Eq. (7) is considered for the plasma parameter $4.0 < f_N/f_H < 4.5$ as indicated by computation (Oya, 1971). If nonlinear coupling does not exist there is no strong dependency on f_N/f_H, for appearance of the signal due to the instability. The second evidence is that as indicated in the record after 0728:00 UT the center frequency of the (3/2) f_H wave decreases continuously toward the outside region of the cyclotron harmonic wave instability. This is possible when the plasma parameter decreases continuously from $f_N/f_H = 2.5$ to $f_N/f_H = 2$ (see Fig. 1). In this region after 0728:04 no cyclotron harmonic wave instability is apparent. This is presumably a tail area of the event where only the wave propagates after the emission from the instability region located in a remote area from the observation points.

4. DISCUSSION AND CONCLUSION

The point to defeat the self consistency of the theory of $2f_H$ wave particle nonlinear interaction including instability of the electrostatic electron cyclotron harmonic wave for the OGO-5 observations is that there is no simultaneous observation of the $2f_H$ wave and that the counter part of the f_{Q3} wave is not constantly observed. The lack of observation of $2f_H$ waves can be attributed to the short length of the dipole antenna compared with the wavelengths (0.5 m for antenna length (Kennel et al., 1970), and hundreds of meter for the electrostatic electron cyclotron harmonic waves). The reception efficiency of the wave with short antenna is inversely proportional to the wave length of the emissions. The wave length of $2f_H$-wave is expanded 10 times or more longer than the f_{D1} wave (Oya, 1970), which correspond to, in this case, the $(3/2)\ f_H$ waves to meet the nonlinear coupling condition given in Eqs. (5) to (7). The energy of $2f_H$ wave that can be picked up by the antenna is possibly reduced by 20 db compared with the energy of the sequence of $(3/2)\ f_H$, $(5/2)\ f_H$ . . . emissions, if the same share of the wave energy is assumed at the three wave decay process. When the value 1-10 mV/m (Kennel et al., 1970) is used for the $(3/2)\ f_H$ wave, the field intensity E of the $2f_H$ wave is $100\ \mu V/m < E < 1\ mV/m$. This is quite the same with the threshold value of OGO-5 receiver (Kennel et al., 1970).

Between 0727:30 and 0727:32 UT in the record given in Fig. 3, the wave which becomes the counter part of f_{Q3} (observed as the case of Alouette-2) is recognized, but usually this wave disappears for the other interval as is the case of $2f_H$ waves; apparently the time duration of f_{Q3} resonance is much less than time durations of these two resonances. Sometimes the f_{Q3} resonance in the Alouette-2 experiment cannot be observed even when f_{D1} and $2f_H$ is clearly revealed. The absence of f_{Q3} resonances directly depend on the parameters other than the natural plasma parameters, and depend on the attitude of the antenna and the satellite velocity vector with respect to the magnetic field, while no such significant dependency is seen for the case of the f_{D1} resonance. All these phenomena are the reflection of the evidence that the f_{Q3} wave is very weak compared with the f_{D1} wave. The attitude change of the antenna and satellite velocity vector from the optimum condition causes the absence of f_{Q3} resonance. In the observation of OGO-5 VLF emission, this situation can be also considered.

In Fig. 4, the plasma parameter is indicated using the result given in Fig. 3 as a final check of the hypothesis that the sequence of $(3/2)\ f_H$, $(5/2)\ f_H$ . . . emissions is caused by the same physical mechanism as the case of sequence of diffuse plasma resonance f_{Dn} except for the initial cause of the plasma turbulence. The range of temperature anisotropy is given to satisfy the limits of the cyclotron harmonic wave instability condition observed from the VLF emission. The plasma parameter f_N/f_H is obtained using the empirical function (see Fig. 1) between f_{Dn}/f_H and f_N/f_H. The error limits given in the diagram corresponds to the width of f_{Dn}/f_H value for a given f_N/f_H. The electron density has been obtained using the obtained f_N/f_H values with the measured f_H frequency which is provided by Heppner's magnetometer (see Fig. 2). The result indicates that OGO-5 encountered a turbulent cloud whose density increases from a value 2×10^{-1}/cc to 5×10^{-1}/cc and drops to about 10^{-1}/cc again. The position in the magnetosphere is given in the figure caption of Fig. 2. The above large density fluctuation was observed in a time interval of about 30 sec which corresponds to a distance of about 100 km along the satellite path. This approach to electron density determination from the sequence of emission of the electrostatic electron cyclotron harmonic waves indicates the same order of density and fluctuation as the ion distribution which are frequently observed in the region $6 < L < 8$ by direct measurements using ion mass spectrometers (Harris et al., 1970, and Chappel et al., 1970).

Considering the established physical mechanism for the f_{Dn} resonance observed on the Alouette-2 and the coincidence of the characteristic points of the frequency range appearance as well as the difference in the experimental setup, we can conclude that the VLF emission detected by Kennel et al. on the OGO-5 satellite data is caused by a turbulence of the plasma in which the electrostatic electron cyclotron harmonic waves are included, as is the case for the f_{Dn} resonances. The only difference between the two experiments is that the turbulence is caused by natural conditions for the VLF emission observed on OGO-5 while the f_{Dn} resonance in Alouette-2 is caused by a stimulating pulse transmission.

ACKNOWLEDGMENTS

I wish to express my sincere thanks to Drs. S. J. Bauer and R. F. Benson for their encouragement, valuable suggestions and support to achieve this work.

REFERENCES

Chappel, C. R., K. K. Harris and G. W. Sharp, The morphology of the bulge region of the plasmasphere, J. Geophys. Res., 75, 3848, 1970.

Hall, L. S., W. Hechrotte and T. Kammash, Ion cyclotron electrostatic instabilities, Phys. Rev. 139, A1117, 1965.

Harris, E. G., Unstable plasma oscillations in a magnetic field, Phys. Rev. Lett., 2, 34, 1959.

Harris, K. K., G. W. Sharp and C. R. Chapell, Observations of the plasmapause from OGO-5, J. Geophys. Res., 75, 219, 1970.

Kadomtsev, B. B., Plasma turbulence, New York: Academic press (Edited by M. G. Rusbridge) 1965, (page 31-35).

Kennel, C. F., F. L. Scarf, R. W. Fredricks, J. H. McGehee and F. V. Coroniti, VLF electric field observations in the magnetosphere, J. Geophys. Res., 75, 6136, 1970.

Oya, H., Sequence of diffuse plasma resonances observed on Alouette-2 ionograms, J. Geophys. Res., 75, 4279, 1970.

Oya, H., Experimental verification of the theory on weak turbulence-interpretation of sequence of diffuse plasma resonance observed in space, Preprint of

Goddard Space Flight Center, Greenbelt, Maryland, X-621-71-22 (accepted by Phys. Fluid) (1971).

Sagdeev, R. Z. and A. A. Galeev, Nonlinear plasma theory, New York: Benjamin Inc., (Edited by T. M. O'Neil) 1969, (page 106).

Shima, Y. and L. S. Hall, Electrostatic instabilities in a plasma with anisotropic velocity distribution, Phys. Rev., 139, A1115, 1965.

Stix, T. H., The theory of plasma waves, New York: McGraw-Hill, 1962.

Terashima, Y., Particle aspect analyses of electromagnetic and electrostatic instabilities due to anisotropic velocity distributions, Progress Theo. Physics, 37, 661, 1967.

Warren, E. S. and E. L. Hagg, Observation of electrostatic resonances of the ionospheric plasma, Nature 220, 466, 1968.

FIGURE CAPTIONS

Figure 1. f/f_H - f_N/f_H diagram of the resonances f_{Dn}, f_{Dn1}, f_{D12}, f_{Qn}, f_N, f_T and nf_H; the cut-off frequencies at the satellite of the x and z propagations are plotted as $f_x S$ and $f_z S$, respectively; on the f_{Dn} resonances, dots indicate the main branch, and open circles and x's indicate the weaker secondary branches at f_{Dn1} and f_{Dn2}, respectively; the open circles with small dots show new data which are added to the originally published data of f_{Dn} and f_{Qn}. (After Oya, 1971.)

Figure 2. The 3/2 f_H, 5/2 f_H and 7/2 f_H observed by OGO-5 satellite near L = 7.5, $\lambda = 1.8°$ and 0053 LT. $f_c/4$,5 $f_c/4$ . . . ($f_c = f_H$) are provided by Heppner's magnetometer (after Kennel et al., 1970).

Figure 3. Normalized frequency band of (3/2) f_H, (5/2) f_H and (7/2) f_H waves using the Kennel's data. Hatched region with dots is a calculated instability domain for $T_\perp/T_\parallel \simeq 5$ and the plain hatched regions are calculated for $T_\perp/T_\parallel \simeq 10$.

Figure 4. Obtained plasma parameters, electron density and temperature anisotropy in a range near L = 7.5, $\lambda = 1.8°$ and 0053 LT.

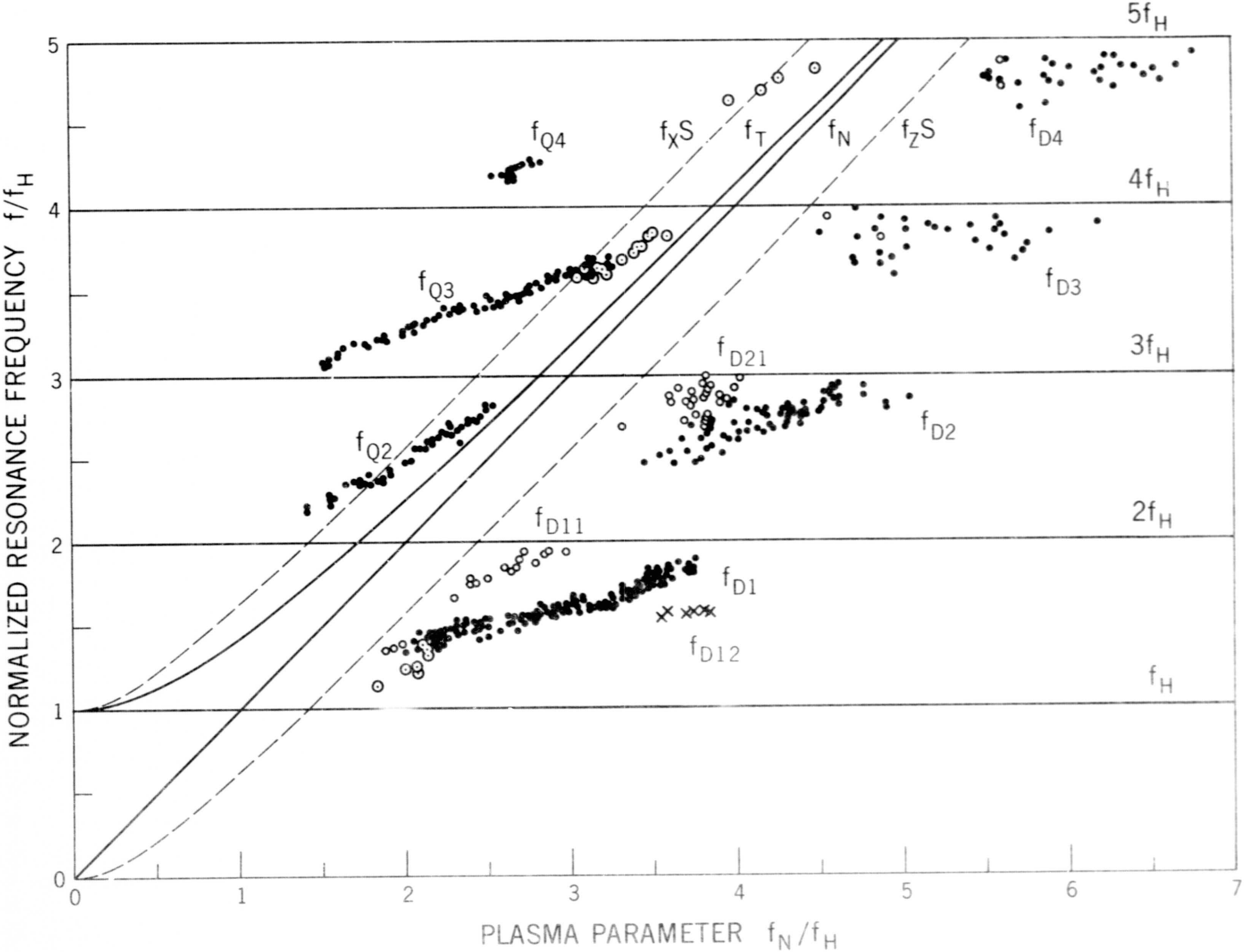

NORMALIZED RESONANCE FREQUENCY f/f_H
PLASMA PARAMETER f_N/f_H
$5f_H$
$4f_H$
$3f_H$
$2f_H$
f_H
f_{Q4}
f_{Q3}
f_{Q2}
f_XS
f_T
f_N
f_ZS
f_{D4}
f_{D3}
f_{D21}
f_{D2}
f_{D11}
f_{D1}
f_{D12}
0
1
2
3
4
5
6
7

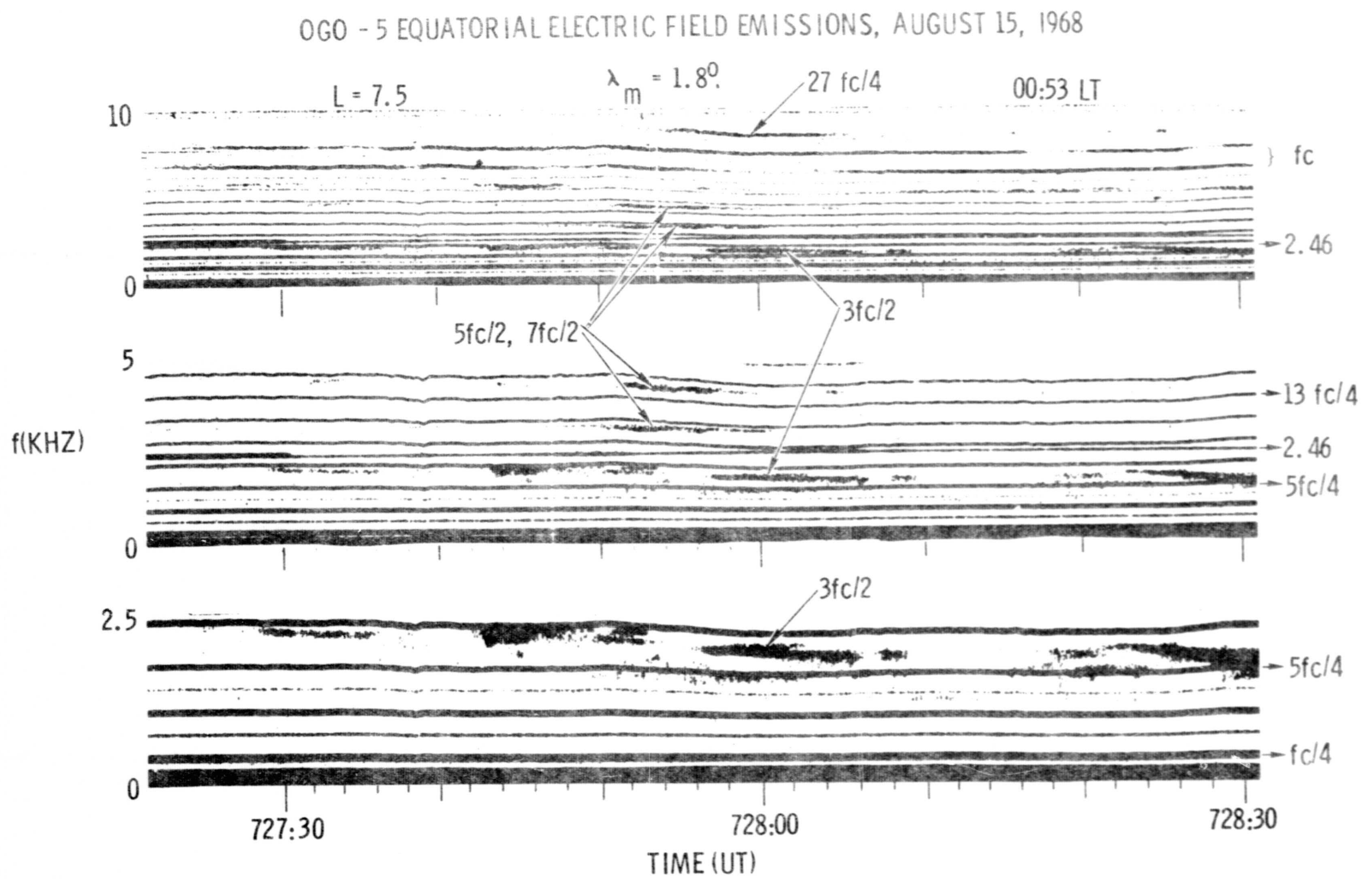
OGO - 5 EQUATORIAL ELECTRIC FIELD EMISSIONS, AUGUST 15, 1968
L = 7.5
λm = 1.8°.
27 fc/4
00:53 LT
10
fc
2.46
0
3fc/2
5fc/2, 7fc/2
5
13 fc/4
f(KHZ)
2.46
5fc/4
0
3fc/2
2.5
5fc/4
fc/4
0
727:30
728:00
728:30
TIME (UT)

Figure 2

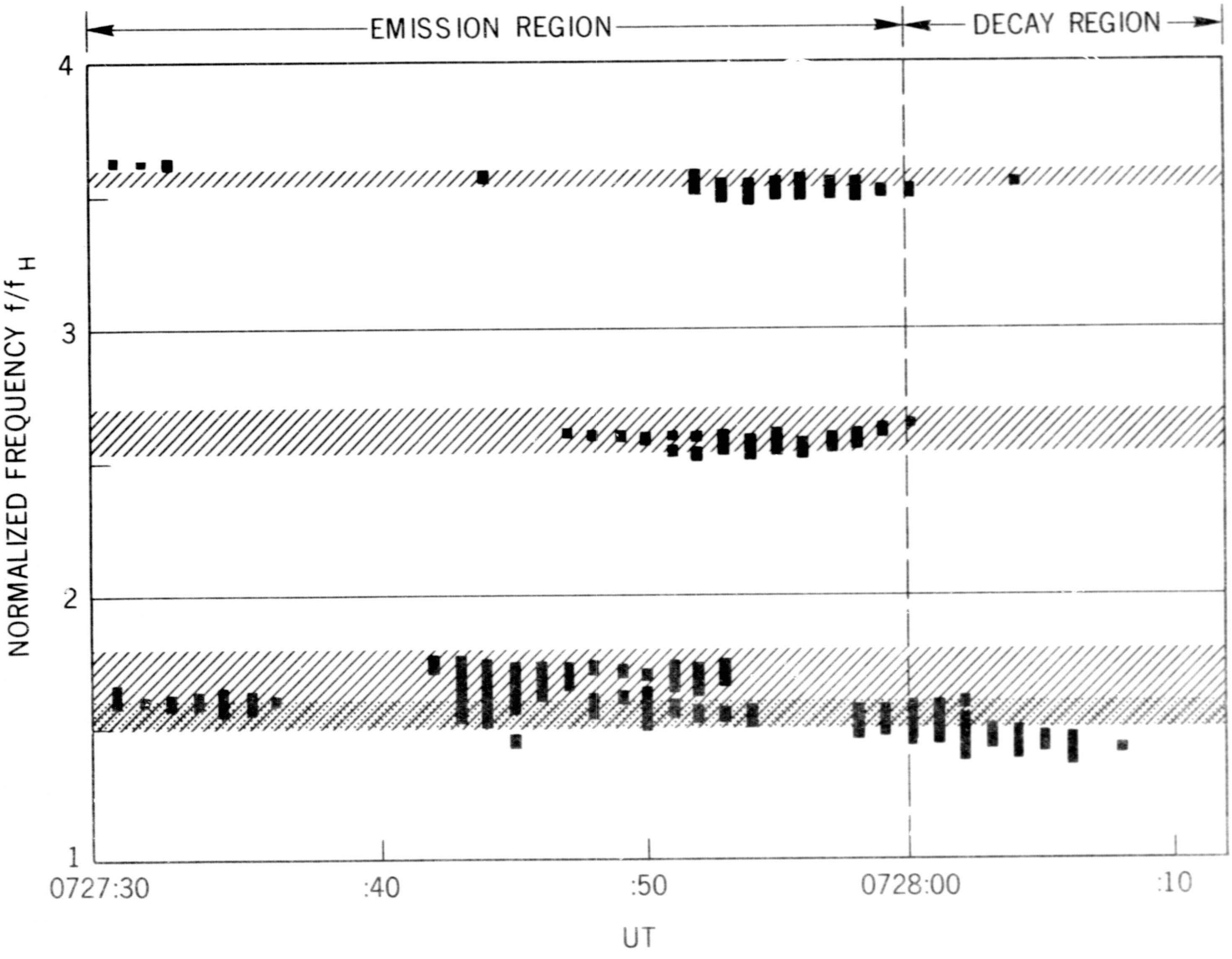

EMISSION REGION
DECAY REGION
4
3
2
1
NORMALIZED FREQUENCY f/f H
0727:30
:40
:50
0728:00
:10
UT

Figure 3

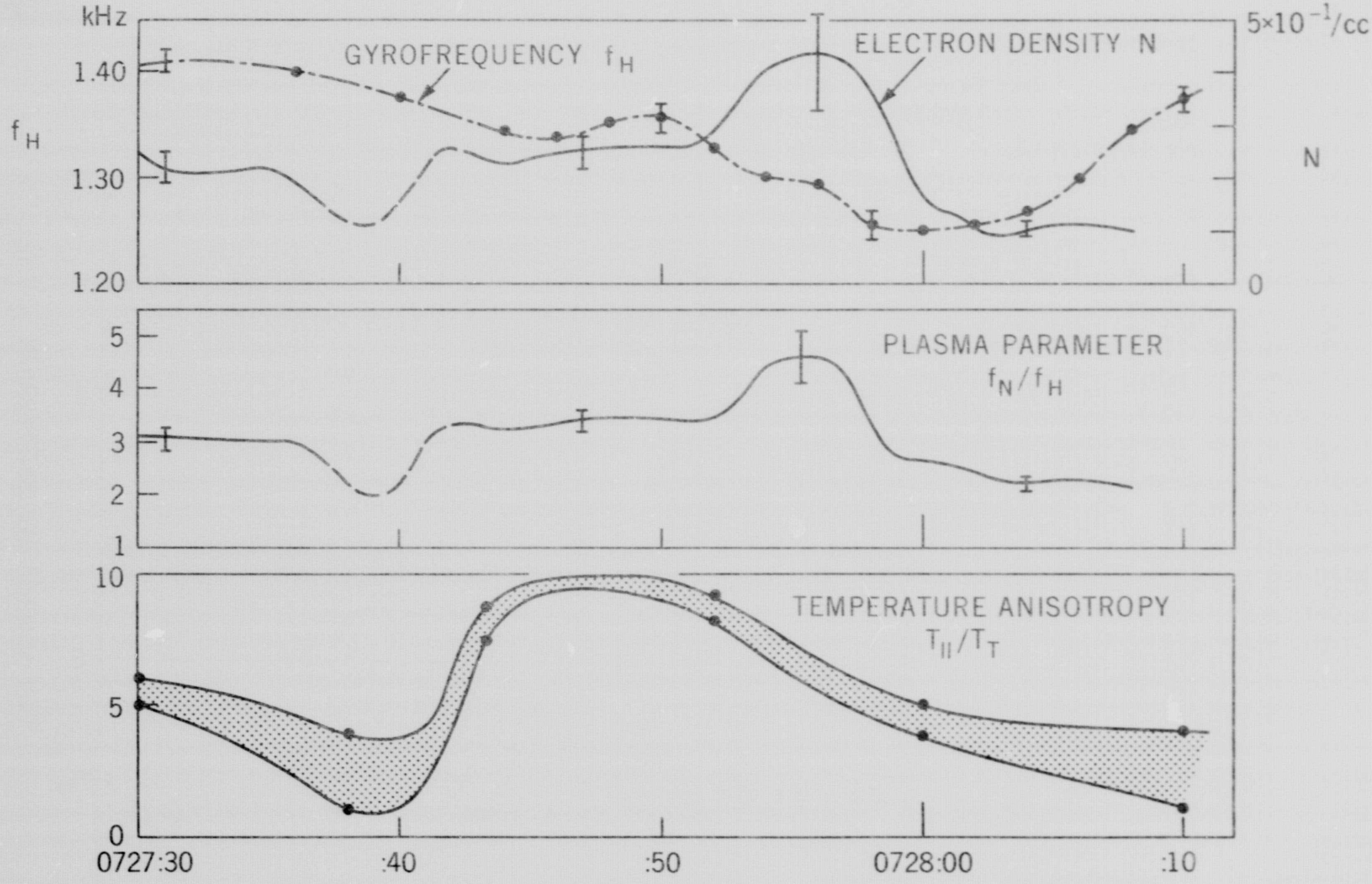
kHz
1.40
1.30
1.20
f_H
GYROFREQUENCY f_H
ELECTRON DENSITY N
5×10^{-1}/cc
N
0
5
4
3
2
1
PLASMA PARAMETER
f_N/f_H
10
5
0
TEMPERATURE ANISOTROPY
T_{II}/T_T
0727:30
:40
:50
0728:00
:10

Figure 4